Cumhuriyet Sci. J., 43(2) (2022) 246-256
DOI: https://doi.org/10.17776/csj.1054772

Cumhuriyet Science Journal

| csj.cumhuriyet.edu.tr | Founded: 2002 ISSN: 2587-2680 e-ISSN: 2587-246X Publisher: Sivas Cumhuriyet University

Computational Structure Characterization of 1,2,3-Selendiazole Isomers, Investigation of Some Molecular Properties and Biological Activities

Sultan Erkan [1,a,*], **Doğan Can Dikyol** [1,b]

[1] *Department of Chemistry, Faculty of Science, Sivas Cumhuriyet University, 58140, Sivas, Türkiye*
**Corresponding author*

Research Article

History
Received: 07/01/2022
Accepted: 09/06/2022

ABSTRACT

Four different selendiazole compounds were handled by computational chemistry methods. Compounds 1,2,3-selendiazole, 1,2,5-selendiazole, 1,2,4-selendiazole and 1,3,4-selendiazole were optimized at the B3LYP/6-31G(d) level. Structural parameters were examined. In the structural determination, IR and NMR techniques, which are spectroscopic methods, were applied. Quantum chemical parameters giving global properties such as the highest occupied molecular orbital (HOMO) energy, the lowest unoccupied molecular orbital (LUMO) energy, hardness (η), softness (σ), chemical potential (μ), electronegativity (χ), electrophilicity index (ω), nucleophilicity index (ε), the electron accepting power (ω^+), electron donating power (ω^-) and polarizability were investigated for biological activities of selendiazoles. Local electrophilic and nucleophilic regions were determined using Fukui index functionals. Docking studies of the studied selendiazoles were performed with proteins representing the cervical cancer cell line and the MCF-7 breast cancer cell line.

Keywords: Selendiazoles, Fukui index, Molecular docking.

[a] *sultanerkan58@gmail.com* *https://orcid.org/0000-0001-6744-929X* [b] *dikyoldogukan@gmail.com* *https://orcid.org/0000-0000-0000-0000*

Introduction

Organoselenium compounds, which are found in trace amounts in nature, contain carbon (C), selenium (Se) and sulfur (S) in their skeleton structure. The two nitrogenous atoms of the mentioned skeletal structure are called selenadiazole. There are basically four known types of selenadiazole heterocycles, with atoms in different positions in the ring structure. These are 1,2,3-selenadiazole with C–Se–N–N bond order, 1,2,4-selenadiazole with N–C–Se–N bond order, 1,2,5-selenadiazole with N–C–Se–C–N bond order and 1,3,4-selenadiazole with N–Se–N bond order given in Figure 1.

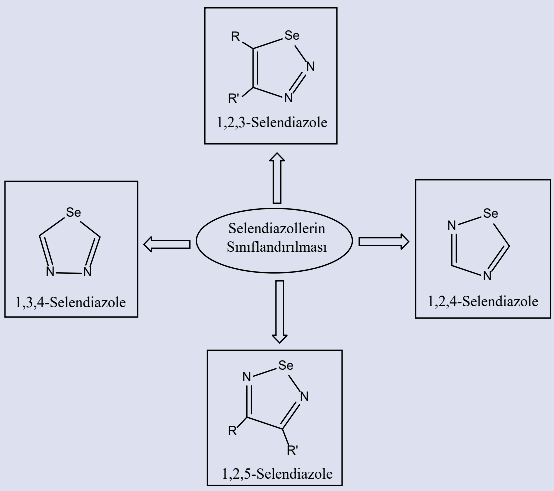

Figure 1. Classification of seleniazoles according to the position of nitrogen and selenium atoms.

1,2,3-Selenadiazoles are a class of selendiazoles whose pharmacological applications have been widely studied. Their derivatives have been evaluated in many studies such as anti-bacterial and anti-cancer [1,2]. The biological activity of 1,2,3-selenadiazoles depends on the electron-accepting and electron-donating properties of the substituents attached to the carbon atoms in the ring structure. As in the nature of most chemicals, differences in functional groups have created differences in their biological potentials. 1,2,3-selenadiazole derivatives act as microbial agents such as antifungal [3], antibacterial [4], antitumor [5], cytotoxic [6] and enzyme inhibitors [7], as well as having important applications in chemotherapy and pharmacology [3-7]. In particular, the benzopyrano-1,2,3-selenadiazole derivatives exhibited antitumor activity against human cell lines such as MCF-7, VERO (African green monkey kidney cells), WI-38 (fibroblast cells) and HEPG-2 (hepatoma cells) [5]. Thioacetanilide derivatives of 1,2,3-selenadiazole showed anti-HIV activity against HIV-1 [6]. There are fewer chemical studies of 1,2,4-selenadiazoles than other selenadiazoles [8-15]. 1,2,5-Selenadiazoles are a type of selenadiazole that contains more information in the literature, thanks to the advantage of the synthesis steps. 1,2,5-selenadiazole compounds exhibit both biological activity and organic light-emitting diode properties [16]. 1,3,4-selendiazoles exhibited physical and biological activity properties on fungi and MAO-B [10]. In addition to these biological properties, organo selenium compounds also act as nonlinear optical potential candidates for electro-optical properties and sensor application [18,19].

In this study, the differences of the basic seleniazole compounds in terms of their structural and molecular properties are discussed. For this purpose, selendiazole compounds are studied by computational chemistry methods. The energy stability of 1,2,3-selendiazole, 1,2,5-selendiazole, 1,2,4-selendiazole and 1,3,4-selendiazole compounds is investigated. For structural analysis, bond lengths, bond angles, differences between IR and NMR data are examined. Quantum chemical parameters are compared to predict the biological activities of the studied compounds. Local eclectrotrophic and nucleophilic regions are determined using the Fukui index functionals. The biological activities of the studied selendiazoles with proteins representing the cervical cancer cell line and the MCF-7 breast cancer cell line are docked with the help of simulation.

Calculation Method

Selendiazole compounds were plotted in the program GaussView 6.0.16 [20]. All calculations were made in Gaussian 09:AS64L-G09RevD.01 program and an imaginary frequency could not be obtained [21]. The B3LYP method was used in the calculations [22-24]. The basis set selection is 6-31G(d) [25].

With the Density Functional Theory, it allows the approximation of quantum chemical descriptors such as hardness (η), softness (σ), chemical potential (μ), and electronegativity (χ). In order to correlate the ground state ionization energy (I) and electron affinity (A) values of chemical compounds, parameters, finite difference approach was considered and finally, the following equations were obtained [26-27].

$$I = -E_{HOMO}$$
$$A = -E_{LUMO}$$
$$\mu = -\chi = \left[\frac{\partial E}{\partial N}\right]_{v(r)} = -\left(\frac{I+A}{2}\right)$$
$$\eta = \frac{1}{2}\left[\frac{\partial^2 E}{\partial N^2}\right]_{v(r)} = \frac{I-A}{2}$$
$$\sigma = 1/\eta$$
$$\omega = \chi^2 / 2\eta = \mu^2 / 2\eta$$
$$\varepsilon = 1/\omega$$
$$\omega^+ = (I+3A)^2 / (16(I-A))$$
$$\omega^- = (3I+A)^2 / (16(I-A))$$
$$\langle \alpha \rangle = 1/3\left[\alpha_{xx} + \alpha_{yy} + \alpha_{zz}\right]$$

In docking studies, compounds and proteins examined in the MMFF94 method were optimized with DockingSever [28]. Charge calculations were made using the Gasteiger method. Neutral media (pH = 7.0) was used in all calculations. The dimensions of the grid maps were 90 × 90 × 90 Å (x, y and z) and were calculated by Solis & Wets local search method and Lamarckian genetic algorithm [29].

Results and Discussion

Optimized Structures

Derivatives of the selendiazoles in the literature, consisting of differences in sulfur, nitrogen and carbon locations, were optimized at the B3LYP/6-31G(d) level. The optimized structures obtained are given in Figure 2. Some bond lengths and bond angles obtained from the optimized structures of seleniazoles are given in Table 1.

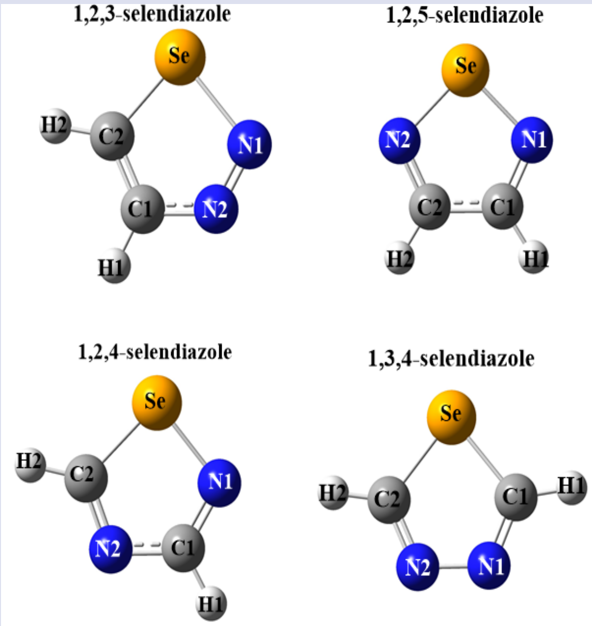

Figure 2. Optimized structures of selendiazoles.

When the bond lengths and angles given in Table 1 are examined, it is generally in the range of 1.845-1.963 Å of Se-C and Se-N bonds. Selenium bonds were found to be the shortest in 1,2,5-selendiazole compound. In 1,2,5-selendiazole, selenium is bonded to two more electronegative nitrogen atoms than carbon. It is expected that nitrogen atoms will attract bond electrons to themselves and the bond they form with selenium is shorter than the others. The lengths of the N-C bonds in the studied compounds are around 1.3 Å. According to the derivatives of the compounds, there is not much difference between C-C bonds and C-H bonds. When their geometric structures are evaluated according to bond angles, there are deviations from the cyclopentadienyl structure.

Table 1. Selected bond lengths and bond angles for selene compounds studied at B3LYP/6-31G(d) level in the gas phase

1,2,3-selendiazole		1,2,5-selendiazole		1,2,4-selendiazole		1,3,4-selendiazole	
Bonds (Å)							
Se-N1	1.963	Se-N1	1.807	Se-N1	1.814	Se-C2	1.872
Se-C2	1.845	Se-N2	1.807	Se-C2	1.867	Se-C1	1.872
N1-N2	1.249	N2-C2	1.310	N1-C1	1.308	C2-N2	1.298
N2-C1	1.381	N1-C1	1.310	C1-N2	1.378	C1-N1	1.298
C1-C2	1.377	C1-C2	1.461	N2-C2	1.302	N1-N2	1.370
C2-C4	1.500	C2-C4	1.503	C1-H1	1.086	C1-H1	1.083
C1-C5	1.504	C1-C3	1.503	C2-H2	1.084	C2-H2	1.083
Bond angles (º)							
Se-N1-N2	108.7	Se-N1-C1	107.8	Se-N1-C1	107.4	Se-C1-N1	114.8
N1-N2-C1	120.0	N1-C1-C2	115.9	N1-C1-N2	122.5	C1-N1-N2	114.4
N2-C1-C2	115.0	C1-C2-N2	115.9	C1-N2-C2	110.3	N1-N2-C2	114.4
C1-C2-Se	110.2	C2-N2-Se	107.8	N2-C2-Se	112.5	N2-C2-Se	114.8
C2-Se-N1	85.84	N2-Se-N1	92.4	C2-Se-N1	87.1	C2-Se-C1	81.4

Stability of Selendiazoles

By examining the thermodynamic parameters of compounds with the same number of electrons, their stability can be predicted. The total energy (E) and Gibbs free energy (G°) taken into account in predicting the stability of the selendizoles were calculated at the B3LYP/6-31G(d) level and are given in Table 2.

Table 2. Total and Gibbs free energies of Selendizoles (kJ·mol^{-1}).

Compounds	E (kJ·mol^{-1})	G° (kJ·mol-1)
1,2,3-selendiazole	-6790280.119660	-6790245.113860
1,2,4-selendiazole	-6790355.014670	-6790316.958053
1,2,5-selendiazole	-6790337.838650	-6790300.519796
1,3,4-selendiazole	-6790281.629322	-6790245.830627

The stability of the Selendiazoles can be determined by decreasing the Total and Gibbs free energies. Selendiazole, which has the lowest energy, has the most stability [30]. Thus, the order of stability of the selendiazoles should be:

1,2,4- elendiazole > 1,2,5-selendiazole > 1,3,4-selendiazole > 1,2,3 -selendiazole

Considering E and G°, the most unstable selendiazole is 1,2,3-selendiazole. However, 1,2,3-selendiazole and 1,3,4-selendiazole E and G° values are close to each other. Therefore, 1,2,3-selendiazole compounds appear in the literature as derivatives too. The 1,2,4-selenadiazoles may have had fewer chemical investigations than other seleniazoles due to their stability.

IR Spectrum

Infrared spectra of molecules are one of the most important methods in structural characterization. The IR spectra of the four derivatives constituting the basic structures of selendiazoles were calculated at the B3LYP/6-31G(d) level. Obtained spectra are given in Figure 2. The peaks in the vibrational spectra of the Selendiazole compounds were numbered. The frequencies in the spectra were examined in detail with the VEDA program and listed in Table 3 and Table 4.

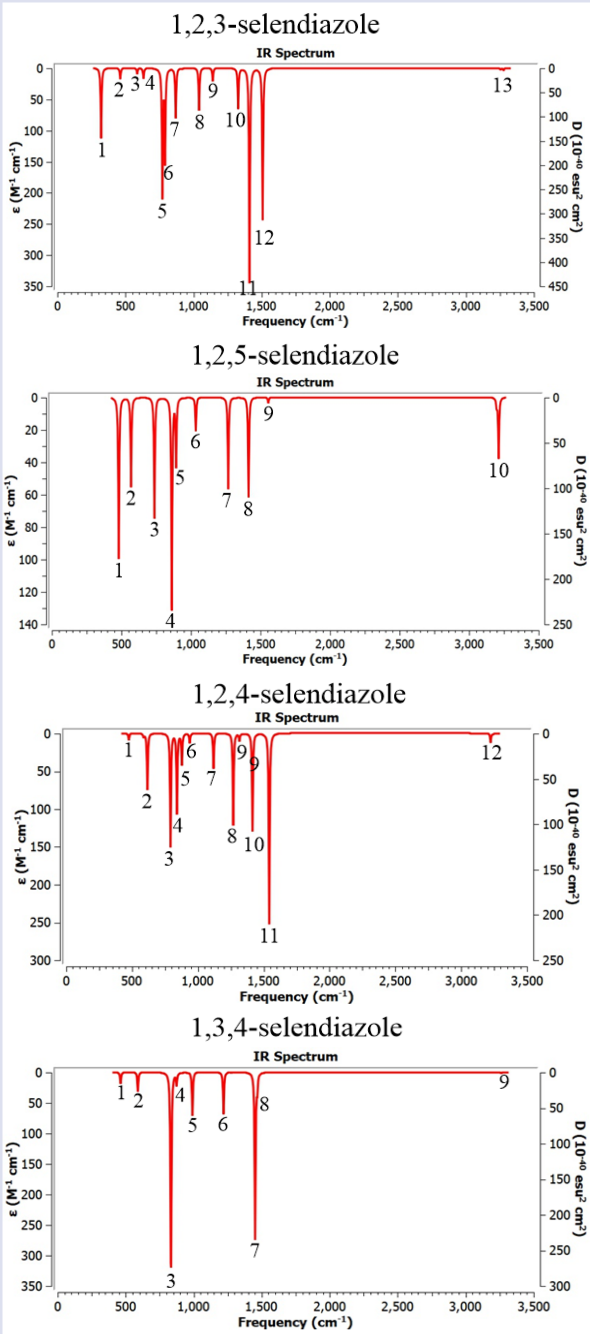

Figure 2. IR spectra of selendiazoles.

Table 3. Calculated frequencies and labeling of 1,2,3 and 1,2,4-selendiazoles

1,2,3 selendiazole			1,2,4 selendiazole		
Mod	Freq. (cm^{-1})	Label	Mod	Freq. (cm^{-1})	Label
1	321	BEND (SeCC) BEND (NNC) BEND (NCC)	1	480	STRE (SeN) BEND (SeNC)
2	461	TORS (NNCC) TORS (NCCSe)	2	616	TORS (CNCN)
3	586	STRE (SeC) BEND (NNC) BEND (NCC)	3	792	BEND (CNC) BEND (NCN) BEND (SeNC)
4	632	TORS (HCNN) TORS (NNCC) TORS (NCCSe)	4	841	TORS (HCNC) TORS (CNCN)
5	771	TORS (HCSeN) TORS (HCNN) TORS (NNCC)	5	878	BEND (CNC) BEND (NCN)
6	790	STRE (SeC) BEND (NNC) BEND (NCC)	6	937	TORS (CNCN)
7	869	BEND (SeCC) BEND (NNC) BEND (NCC)	7	1119	BEND (HCN) BEND (NCN)
8	1040	STRE (NC) BEND (HCSe)	8	1268	BEND (HCN)
9	1141	STRE (CC) STRE (NC) BEND (HCSe) BEND (HCN)	9	1315	STRE (NC) BEND (HCN) BEND (NCN)
10	1327	STRE (NC) BEND (HCSe) BEND (HCN) BEND (NCC)	10	1415	STRE (NC)
11	1411	STRE (NN) STRE (CC)	11	1542	STRE (NC)
12	1507	STRE (NN) STRE (CC) BEND (HCN)	12	3224	STRE (CH)
13	3254	STRE (CH)			

Table 4. Calculated frequencies and labeling of 1,2,5 and 1,3,4-selendiazoles

1,2,5 selendiazole			1,3,4 selendiazole		
Mod	Freq. (cm-1)	Label.	Mod	Freq. (cm-1)	Label
1	480	TORS (SeNCC)	1	460	STRE (SeC) BEND (SeCN)
2	568	STRE (SeN) BEND (SeNC)	2	590	STRE (SeC) BEND (SeCN)
3	737	STRE (CC) BEND (NCC)	3	832	TORS (HCNN)
4	862	TORS (HCNSe)	4	874	BEND (CNN)
5	893	BEND (NCC) BEND (CCN)	5	990	STRE (NN)
6	1035	STRE (CC) BEND (HCN)	6	1219	BEND (HCN)
7	1268	BEND (HCN)	7	1451	STRE (NC)
8	1414	STRE (NC) STRE (CC) BEND (HCN)	8	1467	STRE (NC)
9	1556	STRE (NC)	9	3258	STRE (CH)
10	3212	STRE (CH)			

In Tables 3 and 4, the bond stresses corresponding to the peaks given in the IR spectra of the selendiazoles and their labeling are given. It is seen that the bond stress modes correspond to one or more vibrational transitions with the labels made with the VEDA 4 program, which considers the calculated frequencies potential energy distribution (PED) contributions. Therefore, the high oscillatory strength bond strain modes of the related compounds were investigated. In general, stretching (STRE), bending (BEND) and torsional (TORS) vibrations are also present in selendiazole compounds. Bond stretching frequencies of selenium and selene-bound atoms are at low frequency values. The bond stretch frequencies of 1,2,3-, 1,2,4-, 1,2,5- and 1,3,4-selendiazoles differ slightly from each other. For example, the N-C bond stretching frequency in 1,2,3-selendazole is not alone in the range of 1040, 1141 and 1327 cm^{-1}, but is seen in a peak that includes more than one bond stretching vibrations. C-H bond stretching frequency in 1,2,3-selendazole is 3254 cm^{-1}. The 1,2,4-selendazole compound has only the N-C bond stretching frequency at 1415 and 1542 cm^{-1}. The C-H vibrational frequency for 1,2,4-selendazole is at 3224 cm^{-1}. In the vibration spectrum of 1,2,5-selendazole, the N-C and C-H vibrational spectra correspond to 1556 and 3212 cm^{-1}, respectively. N-C bond stretching frequencies for 1,3,4-selendazole are clearly seen at 1467 and 1451 cm^{-1}. The C-H bond stretching frequency for the mentioned compound is 3258 cm-1.

^{1}H and ^{13}C-NMR Spectrum

NMR spectra of molecules are one of the most essential spectroscopic methods for the identification of skeletal structure. The chemical shifts of the molecules examined by computational chemistry methods were calculated at the B3LYP/6-31G(d) level relative to the reference tetramethylsilane. Atomic labeling and 1H and 13C-NMR spectra of selendiazole compounds are given in Figure 3.

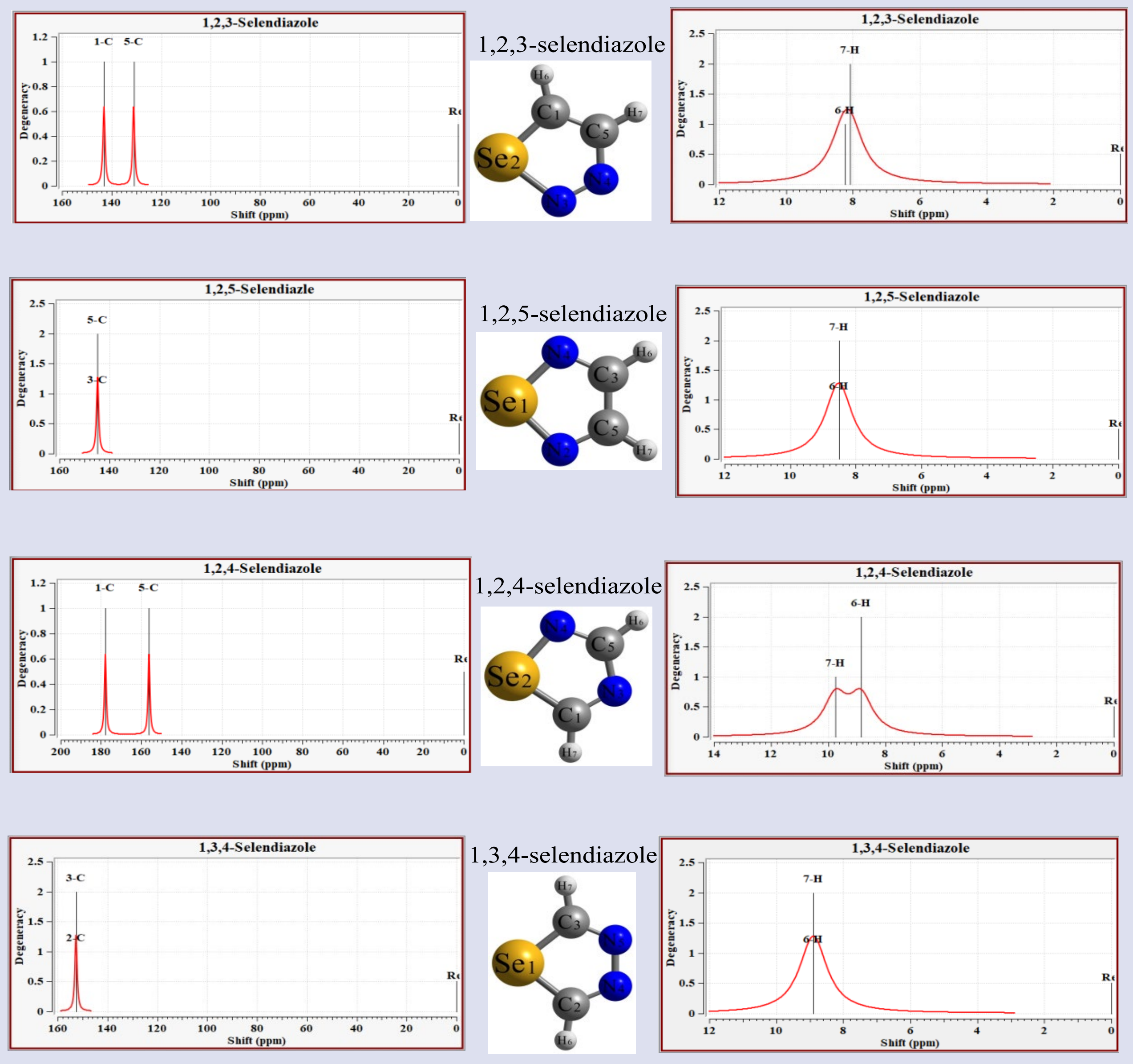

Figure 3. Atomic labeling and ^{13}C- and ^{1}H-NMR spectra of selendiazoles

The data shown in Figure 3 give ^{13}C chemical shifts for the 1,2,3-selendazole molecule. For 1,2,3-selendazole molecule, it is 143.1 and 131.0 ppm at C1 and C5 atoms, respectively. The ^{1}H chemical shifts are 8.2 and 8.1 ppm for H6 and H7 atoms, respectively. ^{13}C chemical shifts for 1,2,5-selendazole molecule were calculated as 144.7 ppm at C3 and C5 atoms. The ^{1}H chemical shifts are 23.5 ppm for the H6 and H7 atoms. The ^{13}C chemical shifts for the 1,2,4-selendazole molecule are 177.8 and 156.1 ppm at the C1 and C5 atoms, respectively. The ^{1}H chemical shifts are 9.7 and 8.8 ppm for H6 and H7 atoms, respectively. ^{13}C chemical shifts for the 1,3,4-selendazole molecule were determined as 152.6 ppm at C2 and C3 atoms. ^{1}H chemical shifts were found to be 8.9 ppm for H6 and H7 atoms. The calculation results meet the theoretical expectations. Nitrogen is an electronegative atom and attracts more electrons than neighboring carbon atoms with lower electronegativity. This results in less shielding of carbon nuclei. Less shielded nuclei exhibit higher chemical shift values. For this reason, there are differences in the chemical shift values of the carbon atoms and subsequently the hydrogen atoms in the molecules.

Quantum Chemical Parameters

Quantum chemical parameters such as the highest occupied molecular orbital (HOMO) energy, the lowest unoccupied molecular orbital (LUMO) energy, hardness (η), softness (σ), chemical potential (μ), electronegativity (χ), electrophilicity index (ω), nucleophilicity index (ε), the electron accepting power (ω+) and electron donating power (ω-) have an important place in biological activity studies. The quantum chemical parameters calculated at the B3LYP/6-31G(d) level for the studied selendiazole molecules are given in Table 5 in detail.

Table 5. Quantum chemical parameters calculated for selendiazole compounds

Parameters	1,2,3-selendiazole	1,2,5-selendiazole	1,2,4-selendiazole	1,3,4-selendiazole
E_{HOMO} (eV)	-6.5969	-6.8146	-7.6647	-7.6114
E_{LUMO} (eV)	-2.0760	-1.8901	-1.7059	-1.8640
ΔE	4.5209	4.9245	5.9588	5.7474
η (eV)	2.2605	2.4622	2.9794	2.8737
σ (eV^{-1})	0.4424	0.4061	0.3356	0.3480
χ (eV)	4.3364	4.3524	4.6853	4.7377
μ (eV^{-1})	-4.3364	-4.3524	-4.6853	-4.7377
ω	4.1595	3.8467	3.6840	3.9054
ε	0.2404	0.2600	0.2714	0.2561
ω^{+}	1.5583	1.4296	1.3323	1.4315
ω^{-}	6.610	6.331	6.399	6.633
α	84.1150	82.9273	57.0193	57.8453

The HOMO and LUMO orbital energies can provide a comparison of the electron-donating and electron-accepting abilities of molecules, respectively. It has been noted that the HOMO orbital represents the electron-donating ability and its high values belong to a good inhibitor. Low LUMO molecular orbital energy and energy gap values between HOMO and LUMO orbitals indicate that the molecule does not want to donate electrons and that electron exchange is easy, respectively. It is clear from the data presented for the energies of the leading molecular orbitals in the table above that the biological activity trends of the studied molecules follow the following order:

1,2,3-selendiazole > 1,2,5-selendiazole > 1,3,4-selendiazole > 1,2,4-selendiazole

Hardness, softness and polarizability, which are among the quantum chemical parameters, can be illuminated in the light of numerical values with electronic structure principles of the molecule's activity behaviors. Chemical hardness is reported as resistance to electron cloud polarization or deformation of molecules [31]. According to Pearson, hard molecules have energy gap values between the high-energy HOMO and LUMO orbitals and are visualized in Figure 4 by contour diagrams. The shapes of the HOMO and LUMO molecular orbitals indicate that the electron-donating orbitals of the compounds are different, but the electron acceptor regions can be generally taken into similar lobes. The global softness of the molecules is equal to the opposite sign of their hardness. Soft and polarizable molecules have high activities. Electronegativity represents the electron-withdrawing forces of molecules and chemical potential electron-donating forces. The electrophilicity index reflects the tendency to accept electrons from electron-rich chemical species. The nucleophilicity index indicates the tendency to donate electrons to chemical species. It can be said that molecules with low electronegativity and electrophilicity index and high chemical potential and nucleophilicity index are more advantageous in terms of biological activities. Moreover, the parameters known as electron donation strength and electron-accepting strength provide important clues about the electron-donating and electron-accepting abilities of molecules. A molecule with effective biological activity should easily donate electrons.

In this case, the activity order of the selendiazoles examined according to the mentioned parameters can be evaluated as follows.

1,2,3-selendiazole > 1,2,5-selendiazole > 1,3,4-selendiazole > 1,2,4-selendiazole

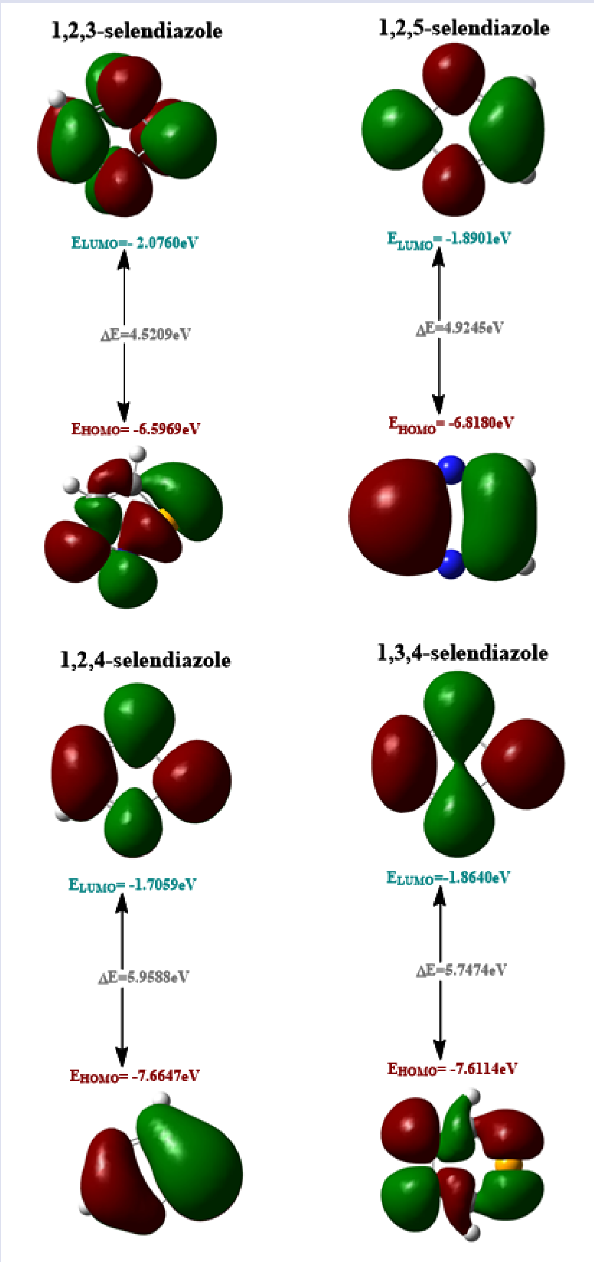

Figure 4. Frontier molecular orbital contour diagrams of selendiazoles

Fukui Indexes

Fukui indices are very important for the analysis of the local atomic activities of Selendiazoles. The calculated Fukui indices of the examined molecules are presented visually in Figure 5. It is important to note that higher f- values represent sites of electrophilic attack, while a higher f+ value corresponds to sites suitable for nucleophilic attack. From the presented image, suitable regions for electrophilic and nucleophilic attacks of the studied molecules can be seen. In addition, electrophilic and nucleophilic indices of atomic-sized selendiazoles are given in Table 6.

Table 6 shows that 4(N) is the most suitable site for electrophilic attack for selendiazole compounds. However, the nucleophilic attack sites of the selendiazole compounds vary according to the derivatives of the compounds.

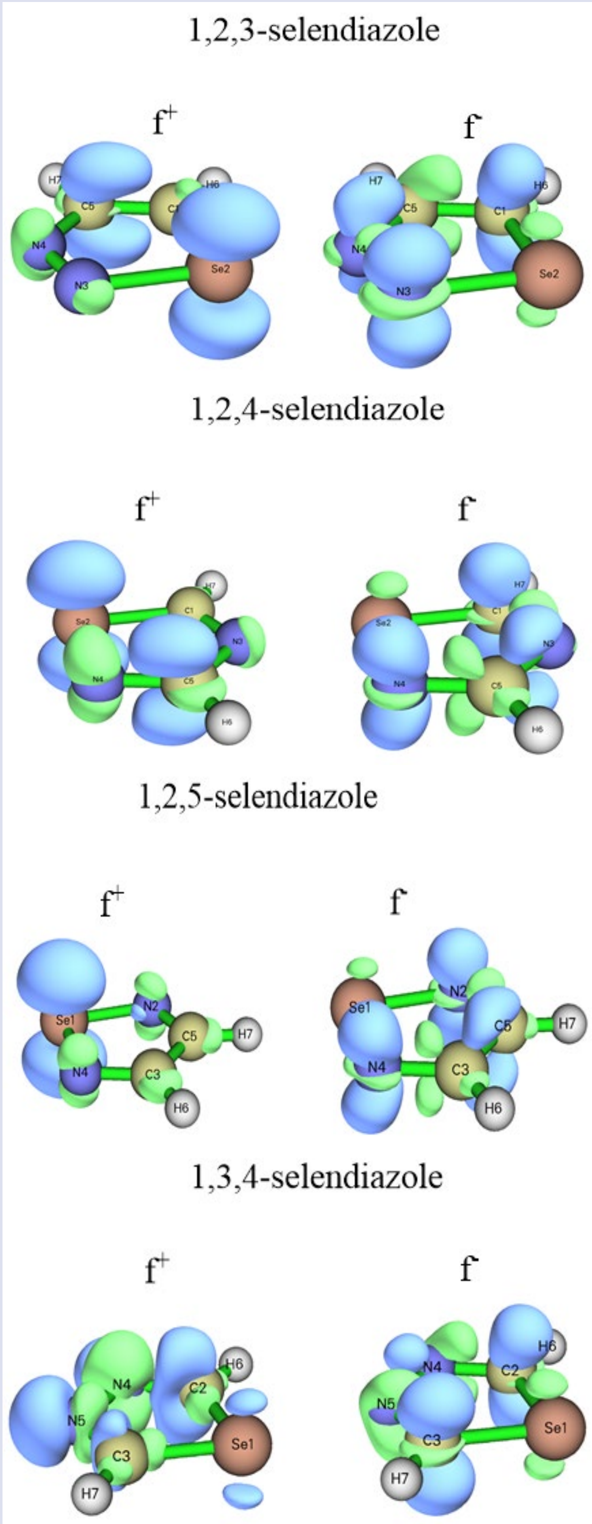

Figure 5. Electrophilic and nucleophilic regions of investigated selendiazoles.

As a result, it has been observed that heteroatoms are the most active atoms. This highlights the important role of selendiazole molecules in their activity and interaction ability.

Table 6. Fukui function indices of the selendiazoles

1,2,3-selendiazole			**1,2,5-selendiazole**		
Atoms	**Electrophilicity**	**Nucleophilicity**	**Atoms**	**Electrophilicity**	**Nucleophilicity**
1(C)	-0.03340	-0.51984	1(Se)	-1.03668	-0.25482
2(Se)	-0.67610	-0.32125	2(N)	-0.00094	-0.55512
3(N)	-0.06783	-0.68865	3(C)	-0.03585	-0.21159
4(N)	0.00095	-0.35577	4(N)	-0.00094	-0.55512
5(C)	-0.31700	-0.00336	5(C)	-0.03585	-0.21159
6(H)	-0.05410	-0.17575	6(H)	-0.06002	-0.11449
7(H)	-0.08148	-0.09374	7(H)	-0.06002	-0.11449
1,2,4-selendiazole			**1,3,4-selendiazole**		
Atoms	**Electrophilicity**	**Nucleophilicity**	**Atoms**	**Electrophilicity**	**Nucleophilicity**
1(C)	-0.02217	-0.57550	1(Se)	-0.43817	-0.29090
2(Se)	-0.74968	-0.27509	2(C)	-0.22625	-0.55817
3(N)	-0.02516	-0.18116	3(C)	-0.11865	-0.55817
4(N)	0.02114	-0.53582	4(N)	0.07060	-0.07091
5(C)	-0.27691	-0.13805	5(N)	-0.28278	-0.07091
6(H)	-0.07471	-0.09915	6(H)	-0.06359	-0.16308
7(H)	-0.05237	-0.17724	7(H)	-0.05620	-0.16308

Molecular Docking

In recent years, molecular docking studies have been very popular in biological activity studies. Thanks to the determined protein sequences of biological systems, the activity studies of the drug candidate molecules examined can be predicted. In this way, information about the interaction energies and binding modes of the biological system with the chemical species can be obtained without loss of time and matter. For this purpose, biological activities of selendiazole derivatives, which basically contain structural differences, against cervical cancer cells and human MCF-7 breast cancer cells were investigated by molecular docking studies. The protein representing the cervical cancer cell line from the protein data bank was identified as PDB ID: 3F81 [32]. Loss of VHR phosphatase induces cell cycle arrest in HeLa carcinoma cells, suggesting that VHR inhibition may be a useful approach to arrest the growth of cancer cells. The 3F81 target protein contains multidentate small molecule VHR inhibitors that inhibit enzymatic activity at anomolar concentrations and exert antiproliferative effects on cervical cancer cells. For the protein representative of the human MCF-7 breast cancer cell line, the target protein PDB ID: 3HY3 [33] was preferred. 5,10-Methenyltetrahydrofolate synthetase (MTHFS) regulates carbon flux through a one-carbon metabolic network that supplies essential components for cell growth and proliferation. Inhibition of MTHFS in human MCF-7 breast cancer cells has been shown to arrest the growth of cells. The lack of three-dimensional structure of human MTHFS (hMTHFS) has hindered the rational design and optimization of drug candidates. The 3HY3 target protein was chosen to examine this deficiency. The interaction energies between selendiazoles and selected target proteins and secondary chemical interactions during binding are given in Tables 7 and 8, respectively. The binding modes obtained from the docking results are given in Figure 6.

Table 7. Docking energies (kcal/mol) between selendizoles and target proteins

Target proteins		3F81			3HY3	
Compounds	E_{BIND}	$E_{SECONDARY}$	E_{TOTAL}	E_{BIND}	$E_{SECONDARY}$	E_{TOTAL}
1,2,3-selendiazol	-4.37	-4.10	-4.37	-4.32	-4.27	-4.32
1,2,5-selendiazol	-3.60	-3.49	-3.60	-3.77	-3.71	-3.77
1,2,4-selendiazol	-3.38	-3.23	-3.38	-3.75	-3.69	-3.75
1,3,4-selendiazol	-4.18	-3.99	-4.18	-4.17	-4.11	-4.17

The energies obtained from the docking results; binding energy (E_{BIND}), secondary chemical interaction energy ($E_{SECONDARY}$) and total interaction energy (E_{TOTAL}). According to these energy values, it is seen that 1,2,3-selendiazole interacts better with the target protein representing the cervical cancer cell line and its biological activity is higher than other selendiazoles. A similar situation shows that the biological activity of 1,2,3-selendiazole compound against the target protein representing the MCF-7 breast cancer cell line is high.

In addition, the results show that there is a general trend in the biological activity ranking of selendiazole.

1,2,3-selendiazole > 1,3,4-selendiazole > 1,2,5-selendiazole > 1,2,4-selendiazole

Table 8. Binding modes between selendizoles and target proteins

Target Proteins	3F81				3HY3			
Compounds	H-bond	Polar	Hydrophobic	Pi-Pi	H-bond	Polar	Hydrophobic	Pi-Pi
1,2,3-selendiazole	CYS124	ARG125 ARG130	-	TYR128	-	-	PRO81 ILE111	-
1,2,5-selendiazole	-	ARG125 ARG130	MET69	-	GLY136 LEU173 GLN178	-	ILE62 PRO135	PHE55
1,2,4-selendiazole	ASP92 CYS124	ASP92 ARG130	CYS124	-	PRO81 PRO112	GLN113	LEU56 PRO81 ILE111	-
1,3,4-selendiazole	CYS124	ARG125 ARG130	-	-			LEU56 PRO81 ILE111	-

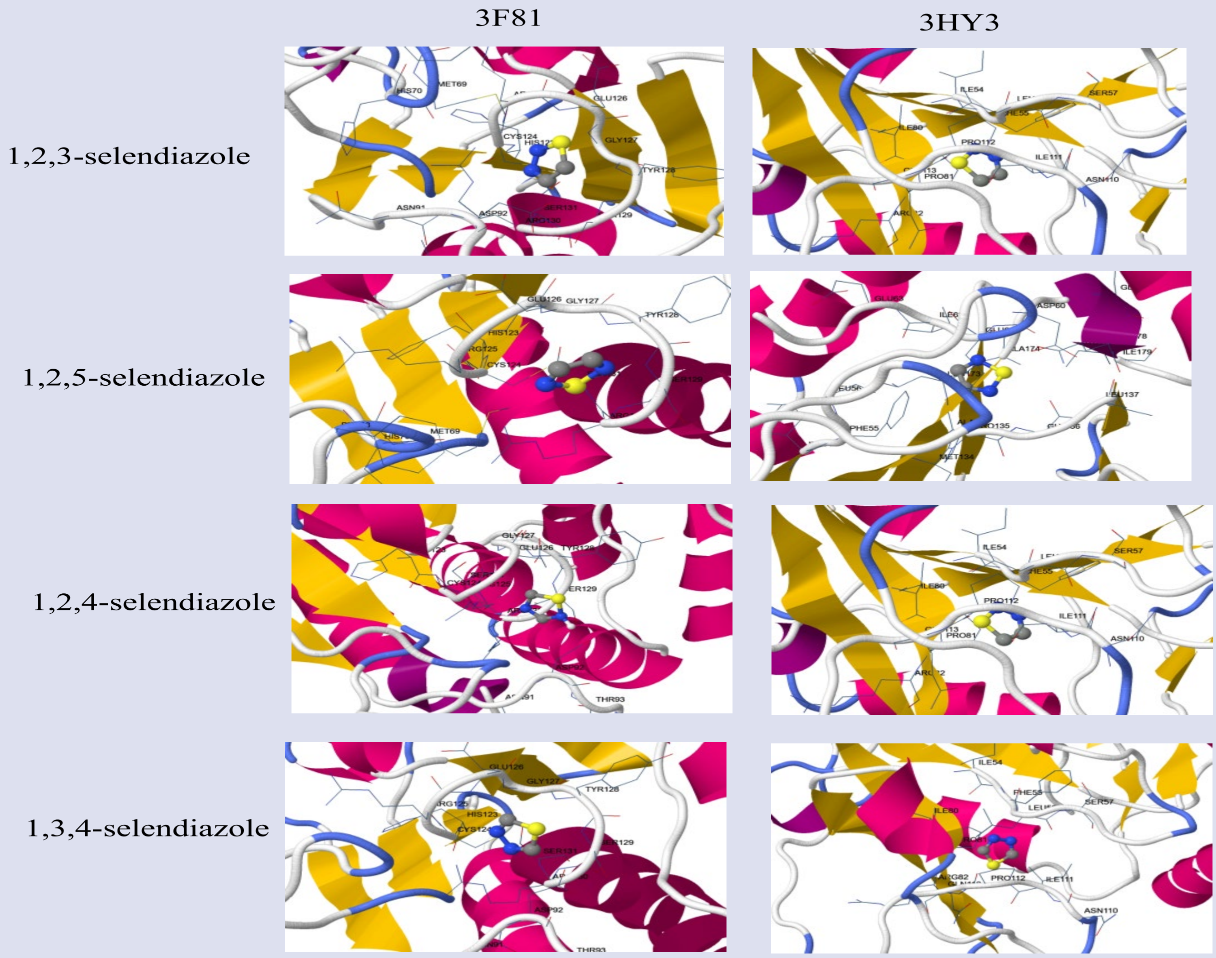

Figure 6. Binding modes between selendiazoles and target proteins.

Conclusion

1,2,3-selendiazole, 1,2,5-selendiazole, 1,2,4-selendiazole and 1,3,4-selendiazole compounds, which are the basic structures of the seleniazole compounds, were optimized at the B3LYP/6-31G(d) level. The obtained structural parameters showed differences in the cyclopentadienyl ring with respect to the selendiazole derivative. The stability of the derivatives of Selendizole compounds was investigated. The most stable structure was determined as 1,2,4-selendiazole and the most unstable structure was 1,2,3-selendiazole. For structural characterization, IR and NMR techniques, which are spectroscopic methods, were applied in detail and the differences between the obtained spectra were compared. Activity estimations were made according to quantum chemical parameters such as the highest occupied molecular orbital (HOMO) energy, the lowest unoccupied molecular orbital (LUMO) energy, hardness (η), softness (σ), chemical potential (μ), electronegativity (χ), electrophilicity index (ω), nucleophilicity index (ε), the electron accepting power (ω^+), electron donating power (ω^-) and polarizability. It is predicted that the activity will increase according to the order of indecision. The local electrophilic and nucleophilic regions were examined using the Fukui index functionals, and the active regions of heteroatoms were obtained from calculations. Selendiazole derivatives were found to exhibit activity parallel to quantum chemical parameters as a result of docking studies with proteins representing cervical cancer cell line and MCF-7 breast cancer cell line.

Conflicts of interest

All authors declare that they have no conflict of interest.

Referanslar

[1] Joshi P. G., More M. S., Jadhav A. A., Khanna P. K., Materials and biological applications of 1, 2, 3-selenadiazoles: a review, *Materials Today Chemistry*, 16 (2020) 100255.

[2] Khanna P. K., Materials chemistry of 1, 2, 3-Selenadiazoles, *Phosphorus, Sulfur, and Silicon and the Related Elements*, 180(3-4) (2005) 951-955.

[3] Moawad E. B., Yousif M. Y., Metwally M. A., Synthesis of certain heteroaryl-fused pyrimidines and pyridines and selena-and thia-diazoles with naphthyl substituent as potential antifungal agents*, Die Pharmazie*, 44(12) (1989) 820-822.

[4] Al-qatrani N. H. K., Essa A. H., Al-Jadaan S. A., Synthesis, Characterization and Antibacterial Activity of Some New 1, 2, 3-Selenadiazole derived from 4-amino acetophenone, *Journal of Physics: Conference Series,* 1279(1) (2019) 012036.

[5] Atta S. M. S., Farrag D. S., Sweed A. M., Abdel-Rahman A. H., Preparation of new polycyclic compounds derived from benzofurans and furochromones. An approach to novel 1, 2, 3-thia-, and selena-diazolofurochromones of anticipated antitumor activities, *European Journal of Medicinal Chemistry*, 45(11) (2010) 4920-4927.

[6] Arsenyan P., Rubin K., Shestakova I., Domracheva I., 4-Methyl-1, 2, 3-selenadiazole-5-carboxylic acid amides: antitumor action and cytotoxic effect correlation. *European Journal of Medicijnal Chemistry*, *42*(5) (2007) 635-640.

[7] Al-Balas Q. A., Al-Smadi M. L., Hassan M. A., Al Jabal G. A., Almaaytah A. M., Alzoubi K. H., Multi-Armed 1, 2, 3-Selenadiazole and 1, 2, 3-Thiadiazole Benzene Derivatives as Novel Glyoxalase-I Inhibitors*, Molecules*, 24(18) (2019) 3210.

[8] Abramov M. A., Dehaen W., D'hooge B., Petrov M. L., Smeets S., Toppet S., Voets M., Nucleophilic intramolecular cyclization reactions of alkynechalcogenolates, *Tetrahedron*, 56(24) (2000) 3933-3940.

[9] Rocha J. B., Piccoli B. C., Oliveira, C. S. (2017). Biological and chemical interest in selenium: a brief historical account*, ARKIVOC: Online Journal of Organic Chemistry*, 2017.

[10] Mhizha S., Młochowski J., Synthesis of 2-acyl-and 2-sulfonylbenzisoselenazol-3 (2H)-ones, *Synthetic Communications*, 27(2) (1997) 283-291.

[11] Fischer H., Kalbas C., Hofmann J., Dichalcogenolanes by ring-expansion of transition metal-coordinated thietanes and selenetanes, *Journal of the Chemical Society*, *Chemical Communications*, (15) (1992) 1050-1051.

[12] Asmus S. M., Bergstraesser U., Regitz M., Organophosphorus compounds; 142: A simple approach to 1, 2, 4-selena-and telluradiphospholes from phosphaalkynes and the chalcogen elements and a first study of their reactivity, *Synthesis,* 1999(09) (1999) 1642-1650.

[13] Ito M., Tokito N., Okazaki R., 1, 3, 2, 4-Diselenastannaboretane, a novel selenium-containing four-membered boracycle: synthesis, structure and thermal cycloreversion into a selenoxoborane*, Chemical Communications*, (22) (1998) 2495-2496.

[14] Kodani M., Takimiya K., Aso Y., Otsubo T., Nakayashiki T., Misaki Y., Effective Synthesis of 1, 3-Diselenole-2-selone-4, 5-diselenolate (dsis) and its Utilization for the Synthesis of Selenocycle-fused Tetraselenafulvalene (TSF) Derivatives*, Synthesis*, 2001(11) (2001) 1614-1618.

[15] Osajda M., Bisbenzisoselenazol-3 (2H)-ones, a new group of ebselen analogues, *Polish Journal of Chemistry*, 75(6) (2001) 823-830.

[16] Bertini V., Synthesis of 1, 2, 5-Selenadiazole and some of its Derivatives, *Angewandte Chemie International Edition in English*, 6(6) (1967) 563-564.

[17] El-Sadek M. M., El-Dayem, N. S. A., Hassan S. Y., Yacout G. A., 1, 3, 4-oxadiazole and selenadiazole derivatives as new C-glycosyl analogs with MAO-B, antibacterial and antifungal activities*, Int. Res. J. Microbiol.*, 4 (2013) 204-219.

[18] Velusamy M., Thomas K. J., Lin J. T., Wen Y. S., Benzo [1, 2, 5] selenadiazole bridged amines: electro-optical properties, *Tetrahedron Letters*, 46(44) (2005) 7647-7651.

[19] Ostrowski J. C., Susumu K., Robinson M. R., Therien M. J., Bazan G. C., Near-Infrared Electroluminescent Light-Emitting Devices Based on Ethyne-Bridged Porphyrin Fluorophores, *Advanced Materials*, 15(15) (2003) 1296-1300.

[20] Dennington R.D., Keith T.A., Millam J.M., GaussView 6.0. 16, Semichem. Inc., *Shawnee Mission* KS, 2016.

[21] Frisch M.J., Trucks G.W., Schlegel H.B., Scuseria G.E., Robb M.A., Cheeseman J.R., Nakatsuji H., Gaussian09 Revision D. 01*, Gaussian Inc.,Wallingford* CT, 2009. http://www.gaussian.com.

[22] Becke A. D., Perspective: Fifty years of density-functional theory in chemical physics, *The Journal of Chemical Physics*, 140(18) (2014) 18A301.

[23] Lee C., Yang W., Parr R. G., Development of the Colle-Salvetti correlation-energy formula into a functional of the electron density, *Physical Review B.*, 37(2) (1988) 785.

[24] Zhao Y., Truhlar D. G., The M06 suite of density functionals for main group thermochemistry, thermochemical kinetics, noncovalent interactions, excited states, and transition elements: two new functionals and systematic testing of four M06-class functionals and 12 other functionals, *Theoretical Chemistry Accounts*, 120(1-3) (2008) 215-241.

[25] Rassolov V.A., Ratner M.A., Pople J.A., Redfern P.C., Curtiss L.A., 6-31G* basis set for third-row atoms, *J. Comput. Chem*., 22 (9) (2001) 976–984.

[26] EL Aatiaoui, A., Koudad, M., Chelfi, T., ERKAN, S., Azzouzi, M., Aouniti, A., & Oussaid, A., Experimental and

theoretical study of new Schiff bases based on imidazo (1, 2-a) pyridine as corrosion inhibitor of mild steel in 1M HCl, *Journal of Molecular Structure*, (2021) 1226 129372.

[27] Al-Otaibi J. S., Mary Y. S., Mary Y. S., Kaya S., Erkan S., Spectral analysis and DFT investigation of some benzopyran analogues and their self-assemblies with graphene, *Journal of Molecular Liquids*, 317 (2020) 113924.

[28] Bikadi Z., Hazai E., Application of the PM6 semi-empirical method to modeling proteins enhances docking accuracy of AutoDock, *Journal of Cheminformatics*, 1(1) (2009) 1-16.

[29] Güzel E., Koçyiğit Ü. M., Taslimi P., Erkan S., Taskin, O. S., Biologically active phthalocyanine metal complexes: Preparation, evaluation of α-glycosidase and anticholinesterase enzyme inhibition activities, and molecular docking studies*, Journal of Biochemical and Molecular Toxicology*, (2021) e22765.

[30] Köse M., Kurtoglu N., Gümüşsu Ö., Tutak M., McKee V., Karakaş D., Kurtoglu M., Synthesis, characterization and antimicrobial studies of 2-{(E)-[(2-hydroxy-5-methylphenyl) imino] methyl}-4-[(E)-phenyldiazenyl] phenol as a novel azo-azomethine dye, *Journal of Molecular Structure,* 1053 (2013) 89-99.

[31] Kaya S., Kaya C., A new method for calculation of molecular hardness: a theoretical study, *Computational and Theoretical Chemistry*, 1060 (2015) 66-70.

[32] Wu S., Vossius S., Rahmouni S., Miletic A. V., Vang T., Vazquez-Rodriguez J., ... Tautz L. Multidentate small-molecule inhibitors of vaccinia H1-related (VHR) phosphatase decrease proliferation of cervix cancer cells*, Journal of Medicinal Chemistry*, 52(21) (2009) 6716-6723.

[33] Wu D., Li Y., Song G., Cheng C., Zhang R., Joachimiak A., ... Liu Z. J., Structural basis for the inhibition of human 5, 10-methenyltetrahydrofolate synthetase by N10-substituted folate analogues, *Cancer Research*, 69(18) (2009) 7294-7301.